JOURNAL OF MATERIALS SCIENCE 16 (1981) 2411–2418

Work-hardening and susceptibility to plastic flow in metallic glasses (rolling deformation)

S. TAKAYAMA
Central Research Laboratory, Hitachi Ltd, Kokubunji, Tokyo, Japan

Fe–Ni-base metallic glass ribbons were rolled "directly" and "indirectly" by changing the rolling direction with respect to the ribbon axis. In the case of direct rolling, no visible deformation bands appeared on the rolling surfaces (except at the edges) but wavy deformation markings appeared on the side surfaces. In the case of indirect rolling, however, the deformation markings developed on the entire surface; they were wavy and straight in appearance on the rolling and side surfaces, respectively. Tensile tests, performed on the samples rolled directly and indirectly show little and much change in fracture stresses, respectively. As a result of the intersecting of plastic flow systems, fracture shear stresses increase by 7% compared with those of as-quenched samples. Fracture shear stresses on a predeformed area were, however, found to be 3% lower than those for an undeformed area. These results are discussed in terms of both work-hardening and work-softening in metallic glasses.

1. Introduction

Following the success of quenching a ribbon metallic sample into an amorphous state, numerous mechanical studies on metallic glasses have been reported [1, 2]. It is well established that (i) a metallic glass has an extremely high strength associated with its rather high ductility, and that (ii) the plastic deformation is highly localized at ambient temperature (inhomogeneous deformation). Furthermore, it has been qualitatively demonstrated that the region previously deformed is susceptible to further plastic flow and preferential etching, suggesting work-softening and a local structural change due to shear stress [3, 4]. On the other hand, the existence of some work-hardening in metallic glasses also has been suggested based on an increase (of about 3%) in hardness with a reduction in thickness for indirect rolling [5]. However, it is still not clear when, or how, such work-hardening or work-softening occurs in metallic glasses.

The aim of the present studies, therefore, was to examine in detail the possibility of work-hardening and work-softening in metallic glasses and to characterize their specific conditions. For this purpose, rolling and subsequent tensile deformation were employed. With regard to rolling deformation, ribbon samples were rolled directly or indirectly between rolls in order to examine the effects of the history of plastic deformation on mechanical properties of metallic glasses, where the terms "indirect" and "direct" denote that a sample is rolled between rollers with and without an assembly sandwiched between stainless steel plates, respectively. In fact, many investigators did not seem to recognize the difference in plastic deformation of metallic glasses due to "direct" and "indirect" rolling. Since the nature of mechanical behaviour in a glassy structure is quite similar over all metallic glasses, the alloys $Ni_{36}Fe_{32}Cr_{14}P_{12}B_6$ (2826A METGLAS) and $Ni_{40}Fe_{40}P_{14}B_6$ (2826A METGLAS) were simply chosen to assess plastic flow after indirect and direct rolling, respectively.

2. Experimental procedure

$Ni_{36}Fe_{32}Cr_{14}P_{12}B_6$ and $Ni_{40}Fe_{40}P_{14}B_6$ alloys, ~ 2 mm wide and $\sim 50\,\mu$m thick, were prepared by rapid quenching from the melt. Ribbon samples were carefully examined by both X-ray and electron diffraction techniques in order to confirm their glassy structures.

In the case of "direct" rolling, samples ~ 25 cm

0022–2461/81/092411–08$02.80/0

in length were cold-rolled between rollers of 130 mm diameter at various directions to the ribbon axis. For "indirect" rolling, however, the ribbon specimens were placed on a stainless steel plate (8 cm x 12 cm) at a desired angle to the rolling direction and sandwiched by another stainless steel plate. These assemblies were then cold-rolled between the same rollers as used above.

For subsequent tensile testing, samples thus deformed were cut into 30 mm lengths and carefully polished by hand using emery paper of the finest particle size to make a gauge section ~ 5 mm in length. In the case of the samples indirectly rolled, both wide surfaces were further polished to 0.03 μm with alumina powder until the deformation bands were completely erased. The aspect ratio (width to thickness) of the gauge section for samples thus prepared was ~ 15. All tensile tests were performed at room temperature at 4×10^{-4} sec^{-1} using an Instron tensile machine.

Deformation bands and fracture surfaces were observed using optical and scanning electron microscopy (SEM).

3. Results

3.1. Indirect rolling

The indirect rolling deformation of metallic glasses has been studied by Takayama and Maddin [5]. They observed deformation markings nearly perpendicular to the rolling direction on the rolling surfaces which were wavy in appearance, whereas those on the narrow side surfaces were relatively straight and inclined at an angle of about 45° to the thickness direction. These deformation markings were also indented on the surfaces of the stainless steel plates sandwiching the sample due to

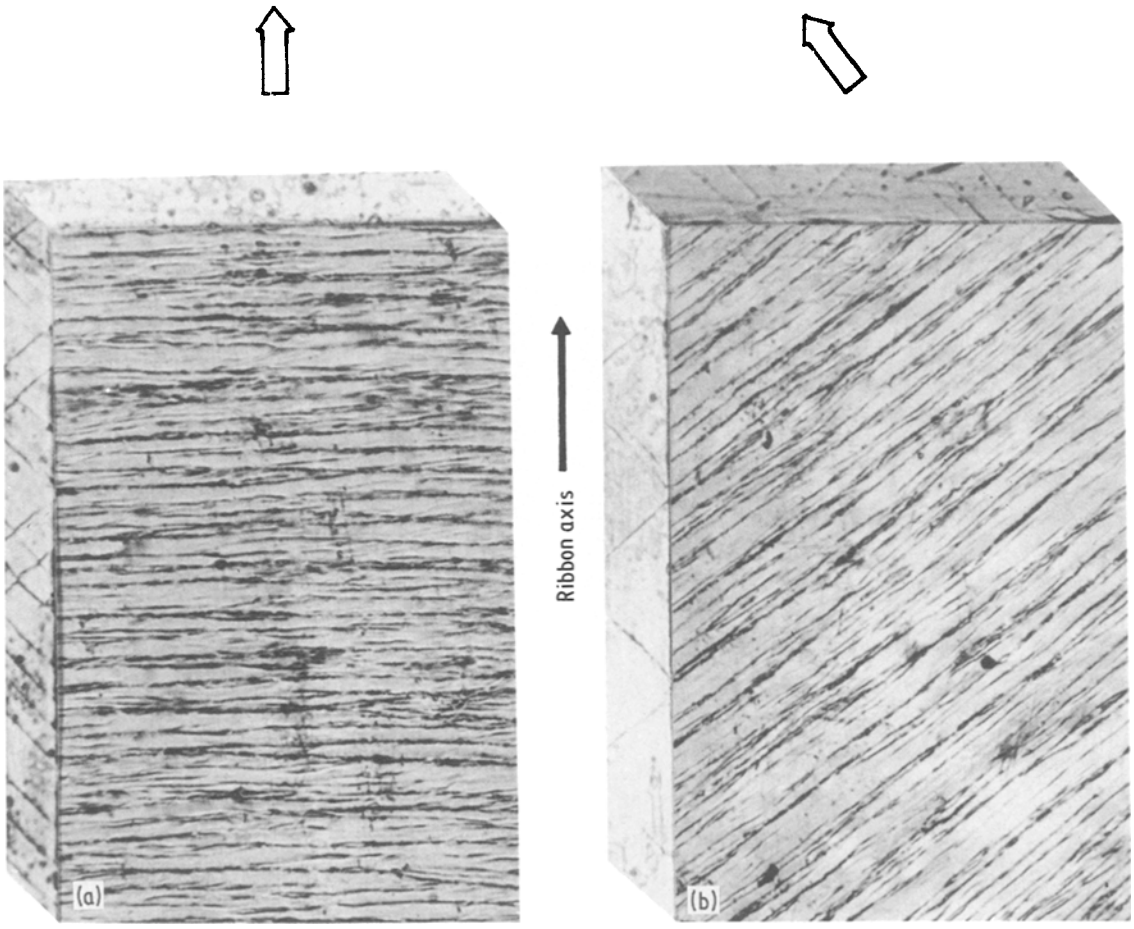

Figure 1 Three-dimensional views of slip patterns for metallic glass $Ni_{36}Fe_{32}Cr_{14}P_{12}B_6$ indirectly rolled to (a) $\epsilon_T = 5\%$ and (b) $\epsilon_T = 7\%$. The arrows indicate a rolling direction.

the lower hardness of the plates compared with that of the metallic glasses. From these results we readily note the following: Since the deformation bands introduced by indirect rolling always appeared perpendicular to the rolling direction on the rolling surfaces, one might produce regular deformation markings making a desired angle on the surfaces with respect to the ribbon axis. This can be done by simply laying a ribbon filament on a stainless steel plate at a desired angle to the rolling direction. Fig. 1 gives the results of such a process where the samples in (a) and (b) were deformed with a 5 and 7% reduction in thickness, ϵ_T, respectively. For the sake of convenience, three-dimensional views of the deformation bands were constructed from optical photographs. The magnifications of the top surface (rolling surface) and the side surfaces are (a) x 80 and (b) x 320. In the photographs, the mismatching of some of the slip lines on both rolling and side surfaces is due to the difference of the magnification and/or the termination of those lines inside the bulk sample. Both arrows in the figure indicate the rolling directions (R.D.). The slip lines make an angle of (a) 90° and (b) 53°35″ to the ribbon axis (0° and 36°25″ to the width axis). It should be emphasized here that the slip planes introduced by indirect rolling are inclined at an angle of 45° to the thickness axis (see the side view of Fig. 1a [5]). Also, one should note that the slip planes introduced as shown in Fig. 1a (i.e. $\theta = 0°$ defined below) become the maximum shear plane for uniaxial tensile stress along the ribbon axis. Hence, for a subsequent tensile test one can readily expect that the samples with $\theta = 0°$ will tend to fail on the pre-existing slip planes due to one of the glassy structure characteristics i.e. work-softening. This is clearly shown below.

The 2826A samples with $\theta = \sim 0°$, $\sim 20°$, $\sim 45°$ and $\sim 55°$, where θ is measured as the angle between the deformation bands and the width axis, were prepared all with the same thickness reduction of $\epsilon_T = \sim 11\%$. Gauge sections of typical tensile specimens exhibiting deformation markings thus introduced are shown on the left hand side of the photographs in Fig. 2a and b; while the corresponding fracture profiles are shown on the right hand side. Note that all samples up to $\theta = \sim 26°$ were fractured along a pre-existing slip line (PSL) (i.e. shear plane), showing a rather sharp edge to the fracture surfaces (Fig. 2a). However, the samples with $\theta = \sim 45°$ began to fail across their widths by shear rupture, cutting through the original deformation bands, and only small portions of the fracture surfaces seem to follow the pre-existing deformation markings. This shear rupture fracture mode became more pronounced for $\theta > \sim 50°$ and such specimens no longer failed along the PSI. This typical fracture profile is shown in Fig. 2b. These resultant fracture stresses are summarized and plotted against θ in Fig. 3, where R.D., R.A. and D denote the rolling direction, ribbon axis and deformation band directions, respectively. The arrows indicate the fracture stress for the unrolled samples (2043 ± 49 MPa (245 ± 5 kg mm^{-1}) an average of seven samples) and the half solid circles show the values for samples fractured along a PSL. The broken line shows the tensile fracture stresses calculated using Equation 1 in Section 4. Fracture stresses increase monotonically with θ. Note that compared with the fracture stresses of unde-

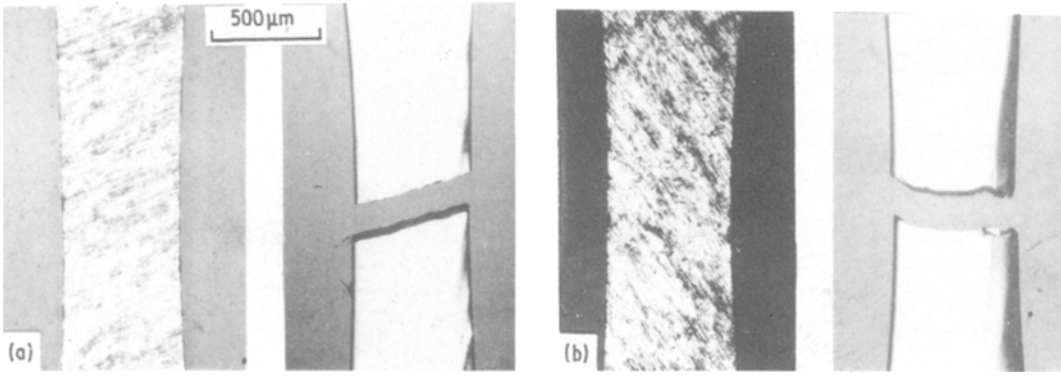

Figure 2 Optical micrographs of 2826A specimens indirectly rolled (a) $\theta = 20°$ and (b) $\theta = 55°$. The left-hand side of the photographs show gauge sections with deformation bands and the right-hand sides show the corresponding fracture profiles.

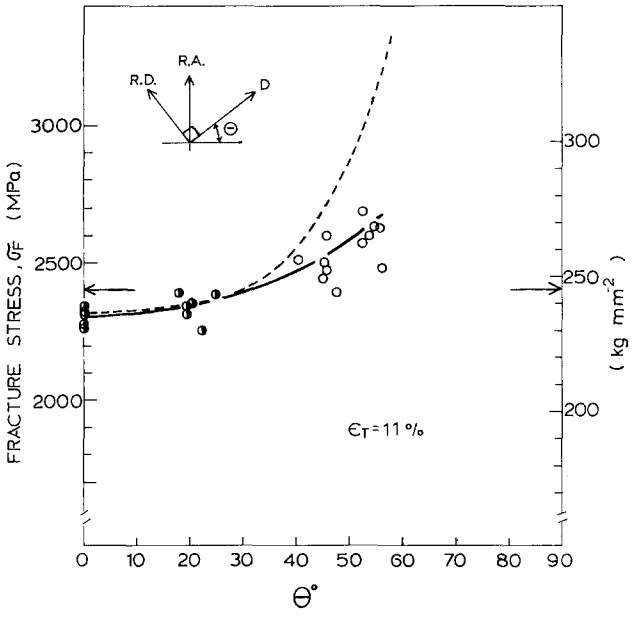

Figure 3 Variation of fracture stress of 2826A samples indirectly rolled with rolling angle θ. R.D., R.A. and D are rolling direction, ribbon axis and deformation band, respectively. The arrows indicate the fracture stress of the as-quenched unrolled samples and the half solids circles show the values for the samples fractured along a pre-existing slip line. The broken line shows the tensile fracture stresses calculated using Equation 1.

formed samples, those of samples which failed along PSLs with $\theta < \sim 40°$ are smaller than those which did not fail along PSLs with $\theta > \sim 40°$ which are larger. These different fracture modes (i.e. cutting and no cutting through the pre-existing slip lines) are also reflected in the fracture morphologies shown in Fig. 4. Fig. 4a and b show the samples rolled with $\theta = 20°$ and 55°, respectively. For the purposes of comparison, the fractography of an unrolled sample is also shown in Fig. 4c. Clearly, the fracture surfaces which failed along a PSL exhibit a large featureless area, indicating a large shear displacement, whereas the fracture surfaces not along a PSL show a large amount of vein patterning associating with a very small featureless part. Comparing the fracture morphologies on the basis of the size vein cell, the size in Fig. 4b is much smaller than that in Fig. 4c. Consequently, these observations allow us to conclude that once the fracture surface cuts through the pre-existed deformation bands, the shear displacement and the size of a vein cell become small, associated with the increase of the fracture stress.

3.2. Direct rolling

Three-dimensional views of the ribbon samples (2826) after direct rolling are shown in Fig. 5. The magnifications of the top and side surfaces are (a) × 28 and (b) × 280. The arrows indicate the rolling directions. The sample of Fig. 5a was deformed at an angle of $\alpha = 0°$ ($\epsilon_T = 19\%$) and

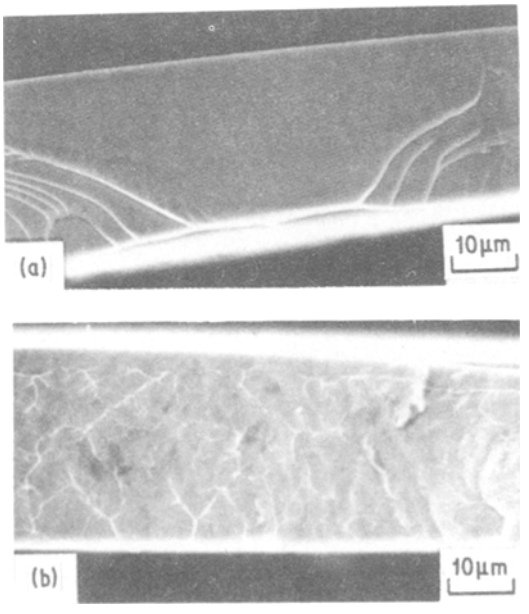

Figure 4 Scanning electron micrographs of the fracture surfaces of 2826A samples rolled indirectly at (a) $\theta = 20°$, (b) 55° and (c) is an unrolled sample.

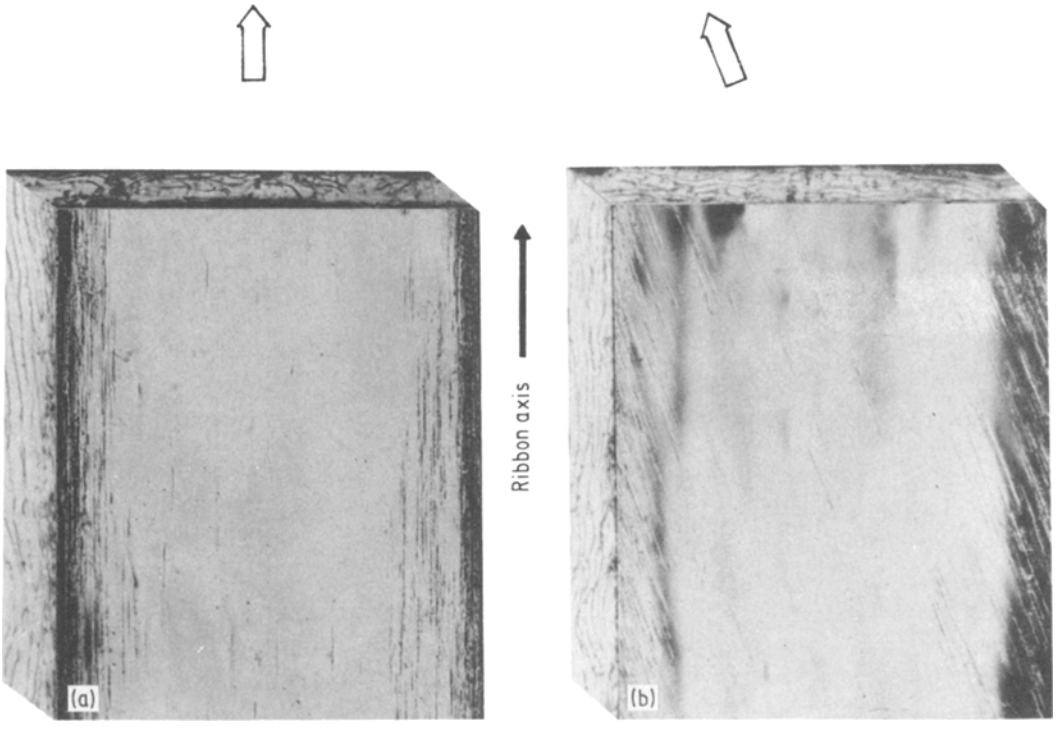

Figure 5 Three-dimensional views of $Ni_{40}Fe_{40}P_{14}B_6$ metallic glass directly rolled with (a) $\epsilon_T = 19\%$ and (b) $\epsilon_T = 18\%$. The arrows indicate the rolling direction.

the sample of Fig. 5b at 16° ($\epsilon_T = 18\%$) where α denotes the angle between the rolling direction and the ribbon axis of the samples. It is apparent that there are striking differences in the appearance of the deformation bands for indirect and direct rolling (compare Fig. 5 with Fig. 1). Note that the lines appearing on the top surfaces in Fig. 5 are not real slip lines, but indented markings caused by the rough surface of the rollers during rolling. Evidently, there are no such distinct deformation bands on the top surfaces, as shown in Fig. 1 (although at higher magnifications, a few wavy slip lines were observed only at the edges of the ribbon sample), but a large number of wavy slip lines are present on the side surfaces. Recalling the fact that slip lines perpendicular to a slip direction are wavy in appearance on metallic glasses [5], the geometric appearance of deformation bands after direct rolling indicates that more likely most of the plastic flow to the rolling surfaces of a sample is supressed during rolling due to the harder material of the rollers compared with the metallic

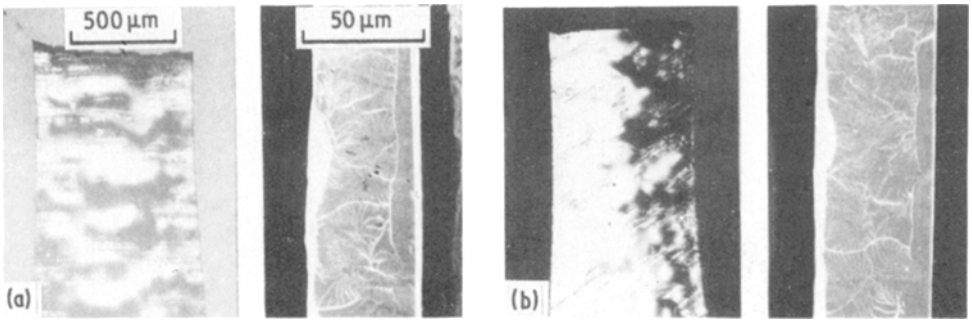

Figure 6 Optical and scanning electron micrographs of the fracture profile (left-hand side) and the corresponding fracture surfaces (right-hand side) of 2926 samples rolled directly at (a) $\alpha = 90°$ and (b) $\alpha = 52°$.

glass, so that plastic flow tends to spread towards the free side surfaces. In effect, such inhibition of plastic flow causes no visible deformation bands on the rolling surfaces, resulting in the appearance of many wavy slip lines on the side surfaces.

The samples thus prepared at the various angles of α with the same thickness reduction $\epsilon_T \sim 25\%$, were also tested in tension. These typical resultant fracture profiles and corresponding fracture surfaces are shown in Fig. 6. Fig. 6a and b denote the samples rolled at $\alpha = 90°$ and 52°, respectively. Note that despite the difference of the rolling angle α, the directly rolled samples fractured in an antiplane strain mode (Mode III) and their fracture morphologies (size of vein cells and featureless portion) are almost the same. Also, the appearance of the fracture morphologies for the rolled samples is almost the same as that for the unrolled samples. This is quite different from the results of indirect rolling (compare Fig. 6 with Fig. 2). The fracture stresses thus obtained are plotted against the angle α in Fig. 7. In the figure, the error bar indicates the standard deviation of five tests and the broken line includes the average fracture stress of the unrolled samples, (2187 ± 10 MPa (223 ± 1 kg mm^{-2}, an average of seven). Contrary to the case of indirect rolling, the fracture stresses show little change with the angle α and are close to the values for the unrolled samples.

Comparing with the samples rolled indirectly between rollers, those rolled directly show little change in mechanical properties and hence appear to be homogeneously deformed. Therefore, it is tempting to conclude that the present direct rolling causes a rather homogeneous deformation on a metallic glass without introducing a macroscopic mechanical anistropy to the ribbon axis, whereas the indirect rolling introduces remarkable anistropy into the samples.

It is important to note, however, that the appearance of deformation bands on the rolling surfaces is largely governed by the relative hardness between a rolled metallic glass and the material used for rolling it. Hence, even in the case of direct rolling, if the material of the roller is weaker than the metallic glass, the result will be the same as in indirect rolling. Likewise, for indirect rolling, if the material of the plates is harder than the metallic glass, the results of direct rolling shown in Fig. 5 or 6 will be expected. Accordingly, whenever discussing the rolling deformation of a metallic glass, one has to specify the type of rolling by which the deformation bands are introduced. Otherwise unnecessary misinterpretation will arise.

4. Discussion

It has been demonstrated that indirect rolling in the present work introduces a salient mechanical anistropy into metallic glasses. To qualitatively estimate the mechanical anistropy, a resolved fracture shear stress, τ_F, has been calculated below. Recalling the discussion by Takayama and Maddin [5] and the actual analysis of three-dimensional observations of slip markings as shown in Fig. 1, the angle made between the normal to the slip plane and the thickness axis can be set as $\pi/4$ for all the samples indirectly rolled. Assuming that the slip direction is the same as the maximum inclined direction of the slip plane (from morphological

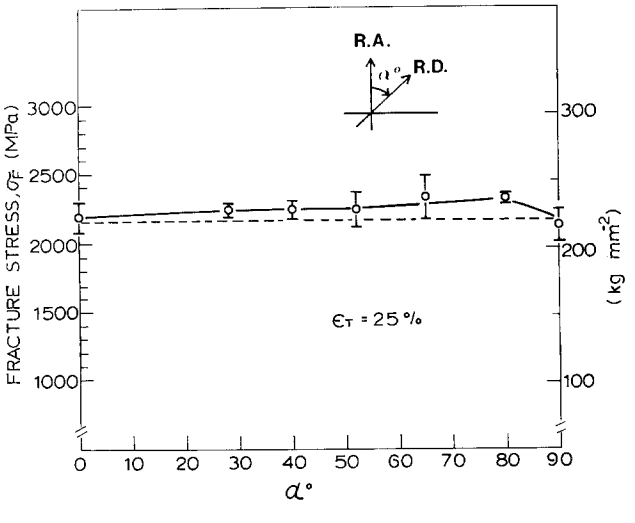

Figure 7 Fracture stress of 2826 samples directly rolled as a function of the rolling angle α.

observations of fracture surfaces, this condition appears to be satisfied in the present cases, see Fig. 4) and τ_F can be expressed as

$$\tau_F = \frac{\sigma_F}{2} \cos\theta \, (2 - \cos^2\theta)^{1/2} \qquad (1)$$

for the samples broken across a PSL ($\theta < 40°$), while, to a good approximation*

$$\tau_F = \sigma_F/2 \qquad (2)$$

for those fractured in Mode III and not along a PSL ($\theta \geqslant 40$). Here θ is the angle between the PSL on the rolling surface and the width axis of a ribbon sample. Resolved fracture shear stresses so obtained by substituting the observed values in Fig. 3 into Equations 1 and 2 are replotted against θ in Fig. 8, where the data values at $\theta = \sim 45°$ were taken only for the samples fractured completely across their widths and not along the PSL. The broken line included indicates the τ_F of the unrolled samples, $\tau_F^0 = 1202\,\text{MPa}(122.5\,\text{kg mm}^{-2})$.

It should be noticed that the shear stress τ_F is approximately constant and increases with θ in the regions below and above $\theta \sim 40°$, respectively. Again, it should be emphasized that when a metallic glass sample fractures across the pre-existing deformation bands, the values of τ_F are larger than those of the unrolled samples τ_F^0, whereas when it is fractured along the PSL, τ_F becomes smaller than τ_F^0. Even taking the data scattering into account, such a decrease or increase in fracture shear stresses, τ_F appears to be significant.

The observed average increase and decrease of τ_F with respect to τ_F^0 are found to be 3 and 7%, respectively, in the regions below and above $\theta \sim 40°$ in Fig. 8. The decrease of τ_F can be readily explained by taking into account one of the characteristics of metallic glasses, i.e. the susceptibility of further plastic flow in a plastically predeformed area (work-softening). This evidence may also be noted from the observation of a large shear displacement on fracture surfaces as shown in Fig. 4a. However, the increase of τ_F cannot be expected from the characteristic of work softening only. Therefore, to interpret this, one has to consider some plastic flow mechanism in a glassy

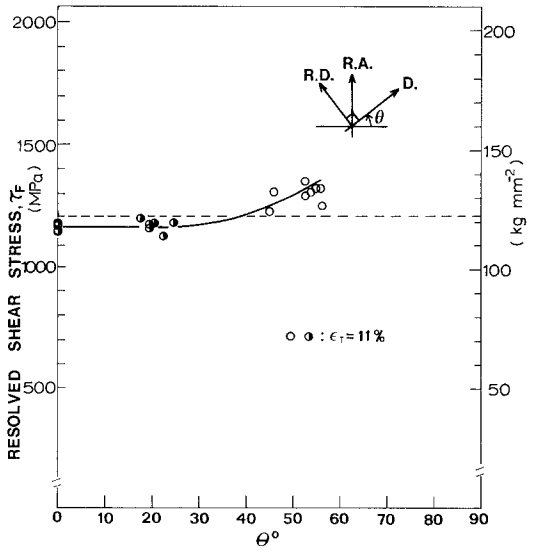

Figure 8 Resolved fracture shear stress τ_F against rolling angle θ. The broken line involved indicates the average resolved fracture shear stress of the unrolled samples.

structure giving rise to the increase of τ_F. Taking account the facts that a localized plastic flow always precedes crack propagation in metallic glasses [6–9] and that the increase of τ_F results from fracture proceeding across pre-existing deformation bands, it appears most likely that a plastically predeformed area plays the role of an obstacle for intersecting plastic flow. In other words, when plastic flow cuts through a predeformed area, it has to overcome the difficulty of additional intersecting. This is a similar phenomenon to the case of work-hardening in a crystalline structure as a result of the interaction between two dislocations. Thus, even in a glassy structure, if the condition of plastic flows intersecting mutually is satisfied, work-hardening results. This evidence also can be confirmed by the drawing and subsequent tensile deformation of $Pd_{77.5}Cu_6Si_{16.5}$ metallic glass wires [4, 10]. The small increase of fracture stresses after direct rolling may also be attributed to this effect. On the basis of the above discussion, the amount of work-hardening and work-softening can be roughly estimated from the increase and the decrease of the shear stress τ_F in Fig. 8. This shows that apparent work-hardening and work-softening in a predeformed area are at

*From the Schmid law, the resolved shear stress τ can be expressed as $\tau = (\sigma/2) \sin 2\chi$, where χ is the angle between the normal to the slip plane and the tensile axis. The observed values of χ at the fracture surfaces of the samples with $\theta \geqslant \sim 45°$ deviate from 40° to 45° and hence the maximum deviation value of $\sin 2\chi$ from $\sin(2 \times \pi/4) = 1$ is only 1.5%.

most 3 and 7% in the present case for $Ni_{36}Fe_2Cr_{14}P_{12}B_6$ metallic glass. Hence, the fracture shear stress on a pre-existing slip plane for $Ni_{36}Fe_2Cr_{14}P_{12}B_6$ metallic glass is founded to be $\tau_F = 1164\,MPa\,(118.7\,kg\,mm^{-2})$ which is 3% lower than that of the unrolled samples. This 3% drop in shear stress in a predeformed area is also in very good agreement with that predicted by Argon [11] assuming a dilatational flow in an amorphous structure. Substituting $\tau_F = 1164\,MPa$ into Equation 1, one can calculate the tensile fracture stress required to fracture on a pre-existing slip plane for various angles of θ. These calculated values are represented by the broken line in Fig. 3. Note that above $\theta = 40°$, the calculated tensile fracture stresses are always greater than those obtained experimentally. Accordingly, at low angles of $\theta\,(<\sim 40°)$, fracture takes place on a pre-existing slip plane owing to work softening. But at a high angle $\theta\,(>\sim 40°)$, the resolved shear stress on a pre-existing slip plane becomes much lower than the resolved shear stress enhanced by work-hardening on a plane of maximum shear stress, so that fracture starts to occur in Mode III.

5. Conclusions

The difference in plastic deformation of metallic glasses after direct and indirect rolling is demonstrated. The mechanical properties of metallic ribbon samples directly and indirectly rolled between rollers were investigated by changing the rolling angle. The results are summarized as follows:

(1) Indirect rolling introduces a large mechanical anistropy into a metallic glass by changing the rolling angle, whereas direct rolling does not.

(2) The conditions required for work-hardening and work-softening to occur in metallic glasses is discussed. It is suggested that work-hardening in a glassy structure takes place when the condition of successive plastic flows intersecting is sufficiently satisfied.

(3) The apparent amount of work-hardening and work-softening are estimated to be at most 3 and 7% for $Ni_{36}Fe_{32}Cr_{14}P_{12}B_6$ metallic glass, respectively, based on the decrease and increase of the resolved fracture shear stress before and after indirect rolling.

Acknowledgement

The author is grateful to the Professor J. C. M. Li for kindly reviewing this paper. This work was performed at both Allied Chemical Corp. (Morristown, NJ) and the University of Pennsylvania (Philadelphia, USA).

References

1. T. MASUMOTO and R. MADDIN, *Mater. Eng.* **19** (1975) 1.
2. J. J. GILMAN, *J. Appl. Phys.* **46** (1975) 1625.
3. C. A. PAMPILLO and H. S. CHEN, *Mater. Sci. Eng.* **12** (1974) 181.
4. S. TAKAYAMA, *Scripta Met.* **13** (1979) 463.
5. S. TAKAYAMA and R. MADDIN, *Acta Met.* **23** (1975) 943.
6. *Idem, Phil. Mag.* **32** (1975) 457.
7. *Idem,* Proceedings of the Second International Conference on Rapidly Quenched Metals, Cambridge, Mass., USA, 1975, Section II (Elsevier, Lausanne, 1975) p. 261.
8. J. MEGUSAR, A. S. ARGON and N. J. GRANT, *Mater. Sci. Eng.* **38** (1979) 63.
9. T. MASUMOTO, *Sci. Rep. RITU* **A26** (1979) 246.
10. S. TAKAYAMA, *Mater. Sci. Eng.* **38** (1979) 41.
11. A. S. ARGON, *Acta Met.* **27** (1979) 47.

Received 16 December 1980 and accepted 11 February 1981.